

## Triaxiality of neutron-rich $^{84,86,88}\text{Ge}$ from low-energy nuclear spectra

M. Lettmann,<sup>1,\*</sup> V. Werner,<sup>1</sup> N. Pietralla,<sup>1</sup> P. Doornenbal,<sup>2</sup> A. Obertelli,<sup>2,3</sup> T.R. Rodríguez,<sup>4</sup> K. Sieja,<sup>5</sup> G. Authalet,<sup>3</sup> H. Baba,<sup>2</sup> D. Calvet,<sup>3</sup> F. Châteaue,<sup>3</sup> S. Chen,<sup>2,6</sup> A. Corsi,<sup>3</sup> A. Delbart,<sup>3</sup> J.-M. Gheller,<sup>3</sup> A. Giganon,<sup>3</sup> A. Gillibert,<sup>3</sup> V. Lapoux,<sup>3</sup> T. Motobayashi,<sup>2</sup> M. Niikura,<sup>7</sup> N. Paul,<sup>2,3</sup> J.-Y. Roussé,<sup>3</sup> H. Sakurai,<sup>2,7</sup> C. Santamaria,<sup>3</sup> D. Steppenbeck,<sup>2</sup> R. Taniuchi,<sup>2,7</sup> T. Uesaka,<sup>2</sup> T. Ando,<sup>2,7</sup> T. Arici,<sup>8</sup> A. Blazhev,<sup>9</sup> F. Browne,<sup>10</sup> A. Bruce,<sup>10</sup> R.J. Carroll,<sup>11</sup> L.X. Chung,<sup>12</sup> M.L. Cortés,<sup>1,2,8</sup> M. Dewald,<sup>9</sup> B. Ding,<sup>13</sup> F. Flavigny,<sup>14</sup> S. Franchoo,<sup>14</sup> M. Górska,<sup>8</sup> A. Gottardo,<sup>14</sup> A. Jungclauss,<sup>15</sup> J. Lee,<sup>16</sup> B.D. Linh,<sup>12</sup> J. Liu,<sup>16</sup> Z. Liu,<sup>13</sup> C. Lizarazo,<sup>1,8</sup> S. Momiyama,<sup>2,7</sup> K. Moschner,<sup>9</sup> S. Nagamine,<sup>7</sup> N. Nakatsuka,<sup>17</sup> C. Nita,<sup>18</sup> C.R. Nobs,<sup>10</sup> L. Olivier,<sup>14</sup> Z. Patel,<sup>11</sup> Zs. Podolyák,<sup>11</sup> M. Rudigier,<sup>11</sup> T. Saito,<sup>7</sup> C. Shand,<sup>11</sup> P.-A. Söderström,<sup>1,2,8</sup> I. Stefan,<sup>14</sup> V. Vaquero,<sup>15</sup> K. Wimmer,<sup>7</sup> and Z. Xu<sup>16,19</sup>

<sup>1</sup>*Institut für Kernphysik, Technische Universität Darmstadt, 64289 Darmstadt, Germany*

<sup>2</sup>*RIKEN Nishina Center, 2-1 Hirosawa, Wako, Saitama 351-0198, Japan*

<sup>3</sup>*CEA, Centre de Saclay, IRFU/Service de Physique Nucléaire, 91191 Gif-sur-Yvette, France*

<sup>4</sup>*Departamento de Física Teórica, Universidad Autónoma de Madrid, 28049, Spain*

<sup>5</sup>*IPHC, CNRS/IN2P3 et Université de Strasbourg, 67037 Strasbourg, France*

<sup>6</sup>*State Key Laboratory of Nuclear Physics and Technology, Peking University, Beijing 100871, P.R. China*

<sup>7</sup>*Department of Physics, University of Tokyo, 7-3-1 Hongo, Bunkyo, Tokyo 113-0033, Japan*

<sup>8</sup>*GSI Helmholtzzentrum für Schwerionenforschung GmbH, 64291 Darmstadt, Germany*

<sup>9</sup>*Institut für Kernphysik, Universität zu Köln, 50937 Köln, Germany*

<sup>10</sup>*School of Computing Engineering and Mathematics,*

*University of Brighton, Brighton BN2 4GJ, United Kingdom*

<sup>11</sup>*Department of Physics, University of Surrey, Guildford GU2 7XH, United Kingdom*

<sup>12</sup>*Institute for Nuclear Science & Technology, VINATOM, P.O. Box 5T-160, Nghia Do, Hanoi, Vietnam*

<sup>13</sup>*Institute of Modern Physics, Chinese Academy of Sciences, Lanzhou 730000, P.R. China*

<sup>14</sup>*Institut de Physique Nucléaire Orsay, IN2P3-CNRS, 91406 Orsay Cedex, France*

<sup>15</sup>*Instituto de Estructura de la Materia, CSIC, 28006 Madrid, Spain*

<sup>16</sup>*Department of Physics, The University of Hong Kong, Pokfulam, Hong Kong*

<sup>17</sup>*Department of Physics, Faculty of Science, Kyoto University, Kyoto 606-8502, Japan*

<sup>18</sup>*Horia Hulubei National Institute of Physics and Nuclear Engineering (IFIN-HH), 077125 Bucharest, Romania*

<sup>19</sup>*KU Leuven, Instituut voor Kern- en Stralingsfysica, 3001 Leuven, Belgium*

(Dated: February 3, 2017)

$\gamma$ -ray transitions between low-spin states of the neutron-rich  $^{84,86,88}\text{Ge}$  were measured by means of in-flight  $\gamma$ -ray spectroscopy at 270 MeV/u. Excited  $6_1^+$ ,  $4_{1,2}^+$  and  $2_{1,2}^+$  states of  $^{84,86}\text{Ge}$  and  $4_1^+$  and  $2_{1,2}^+$  states of  $^{88}\text{Ge}$  were observed. Furthermore a candidate for a  $3_1^+$  state of  $^{86}\text{Ge}$  was identified. This state plays a key role in the discussion of ground-state triaxiality of  $^{86}\text{Ge}$ , along with other features of its low-energy level scheme. A new region of triaxially deformed nuclei is proposed in the Ge isotopic chain.

Since the early days of nuclear structure physics, nuclei of triaxial shape are a subject of high interest. In the 1950s two elementary models were derived, which include a breaking of the axial symmetry of the Bohr Hamiltonian [1] by introducing the triaxial deformation parameter  $\gamma$ . The rigid triaxial rotor model by Davydov and Filippov [2] considers a well defined minimum for a certain value of  $\gamma$  in the potential energy surface while the model by Wilets and Jean [3] treats the potential independently of  $\gamma$ , called  $\gamma$ -soft. More microscopic models, such as the shell model [4, 5], the algebraic interacting boson model (IBM) [6], mean field approaches (e.g., [7]) or energy density functional based models (e.g., [8]), discuss potential energy surfaces in terms of the geometrical deformation parameters  $\beta$  and  $\gamma$ .

The discussion of triaxiality in nuclei covers various regimes of angular momenta. At high spins, quasi-particle configurations or so-called wobbling modes (e.g., [9–11]) have been found to be the basis of triaxial super-

deformed bands. At intermediate spins, there has been much discussion about chirality in odd-odd nuclei [12–14], based on the spin axes of the unpaired proton and neutron, and the rotational axis of the core. However, in this regime, in some cases there has been controversy as to the rigidity or softness of the nuclear body leading to the observed structures [15]. At the lowest spins, however, especially in the ground state itself, triaxial structures have typically been ascribed to pronounced  $\gamma$ -softness, corresponding to a broad minimum in  $\gamma$ . This type of nuclei closely relates to the O(6) dynamical symmetry limit of the IBM-1, with the best known example being  $^{196}\text{Pt}$  [6, 16–18].

The low-spin spectra formed by a triaxial rigid rotor and a  $\gamma$ -soft nucleus exhibit rather similar features. Most importantly, the band head of the (quasi-) $\gamma$  band is positioned at low energy, typically below the yrast- $4^+$  state. This is distinct from the comparatively high energies of the  $\gamma$  band in axially-symmetric rotors, as found, e.g.

in neutron-rich Ar isotopes [19]. A significant difference between the soft and rigid cases is the energy spacing between the odd and even members of the  $\gamma$  band, i.e., the distance of the  $3_2^+$  state to the  $2_1^+$  and  $4_1^+$  states. In the case of a triaxial rigid rotor, the odd-spin levels are located closer to the lower-lying even spin levels, whereas the odd spin levels are closer to the higher-lying even spin levels in the case of a  $\gamma$ -soft nucleus. This relative location of even and odd spin states is usually referred as staggering [20, 21]. The only experimental evidence over the entire nuclear chart for a significant degree of rigid triaxiality in the ground state was recently provided by Toh *et al.* [22] for the nucleus  $^{76}\text{Ge}$ .

Besides the experimental confirmation of triaxiality in  $^{76}\text{Ge}$ , various calculations were performed for even-even germanium isotopes from stability toward the magic neutron number  $N = 50$ . These calculations predict this region to be dominated by  $\gamma$ -soft nuclei with only one isolated case of a rigid triaxial deformed nucleus which is either  $^{74}\text{Ge}$  [23–25] or  $^{76}\text{Ge}$  [26]. Furthermore, it was shown that a new region of rigid triaxial deformation should arise around  $N = 54$ , which is supported by shell model and beyond-mean-field calculations [27, 28], predicting a maximum of triaxiality for the exotic nucleus  $^{86}\text{Ge}$ . Also in the broader mass region above  $N = 50$ , new Monte-Carlo shell model calculations [29] predict the occurrence of coexisting prolate and triaxial shapes, e.g., leading to a low-lying triaxial band in  $^{110}\text{Zr}$  at  $N = 70$ . For proton numbers between  $Z = 28$  and 40 the  $N = 56, 58$  sub-shell closures ( $2d_{5/2}, 3s_{1/2}$ ) may diminish, possibly leading to the occurrence of triaxial structures at smaller values of  $N$  as compared to the chain of zirconium isotopes. Nevertheless,  $N = 56, 58$  may still have a stabilizing influence. The prediction of a region of triaxiality in neutron-rich germanium isotopes is backed by further systematic theoretical studies [30, 31]. The present work aims at providing experimental benchmarks from  $\gamma$ -ray spectroscopy on the neutron-rich Ge isotopes up to  $N = 56$ .

An experiment was conducted at the Radioactive Isotope Beam Factory (RIBF) [36, 37] at Tokyo. A  $^{238}\text{U}$  beam with an energy of 345 MeV/u impinged on a 3 mm thick  $^9\text{Be}$  target at the entrance of the BigRIPS fragment separator [38]. The isotopes of interest were produced by in-flight fission, selected by the  $B\rho - \Delta E - B\rho$  method and identified on an event-by-event basis by the  $\text{TOF} - B\rho - \Delta E$  method in BigRIPS [39]. Data was taken in two different BigRIPS settings.  $^{87}\text{As}$  and  $^{85}\text{Ge}$  were obtained with rates of  $2059\text{ s}^{-1}$  and  $731\text{ s}^{-1}$ , respectively, in one setting of 22 hours. In a second setting of 10.5 hours,  $^{89}\text{As}$  was provided with a rate of  $140\text{ s}^{-1}$ . The isotopes of interest impinged on the 99(1) mm thick liquid hydrogen reaction target MINOS [40], at the end of the BigRIPS fragment separator. The ions kinetic energy of  $\sim 270\text{ MeV/u}$  was reduced by  $\sim 70\text{ MeV/u}$  while passing the target. Products from secondary (p,2p) or (p,pn)

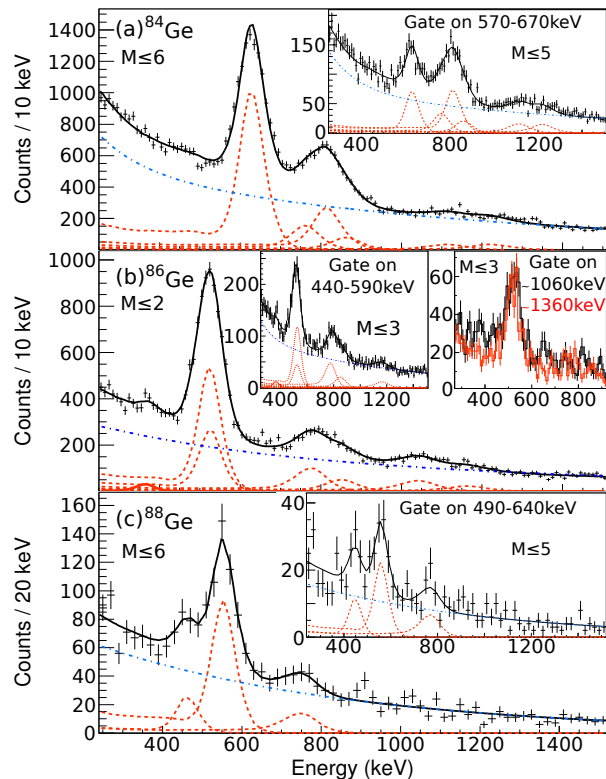


FIG. 1: Three different reaction channels are shown: (a)  $^{85}\text{Ge}(p,pn)^{84}\text{Ge}$ , (b)  $^{87}\text{As}(p,2p)^{86}\text{Ge}$ , (c)  $^{89}\text{As}(p,2p)^{88}\text{Ge}$ . The Doppler-corrected  $\gamma$ -ray spectrum is shown by the black data points. The simulated lineshape of the whole spectrum (black solid line) is composed of a two-exponential function describing the background (blue dash dotted line) and the simulated response function of DALI2 for each transition (red dotted line) fitted to the data points. Spectra after gating on the regions of the  $2_1^+$  states are shown in the insets. In panel (b) gates on the region of the  $2_2^+ \rightarrow 0_1^+$  transition (black) and a neighboring region (red) are shown in addition.  $M$  denotes the multiplicity cutoff and is chosen to optimize the balance of background to peak according to available statistics. For  $^{84}\text{Ge}$  higher  $M$  is chosen to enhance higher-lying transitions.

reactions in the  $\text{LH}_2$  target were identified by the ZeroDegree spectrometer [38] by applying the  $B\rho - \Delta E - B\rho$  method. The vertices of these reactions were determined by a time projection chamber (TPC) surrounding the  $\text{LH}_2$  target. De-excitation  $\gamma$ -rays were observed in the NaI(Tl) scintillator array DALI2 [41] covering polar angles from 10 to 128 degrees with respect to the central beam axis and to the center of MINOS. By a simulation within the GEANT4 framework [42], a full-energy peak detection efficiency of 35% and 23% was obtained for a 500 keV and 1 MeV  $\gamma$ -ray (with addback) emitted from a nucleus at the center of the target with a kinetic energy of 250 MeV/u. The energy calibration was done with five transitions from  $^{137}\text{Cs}$ ,  $^{88}\text{Y}$  and  $^{60}\text{Co}$  sources ranging from 662 keV to 1.836 MeV. A calibration er-

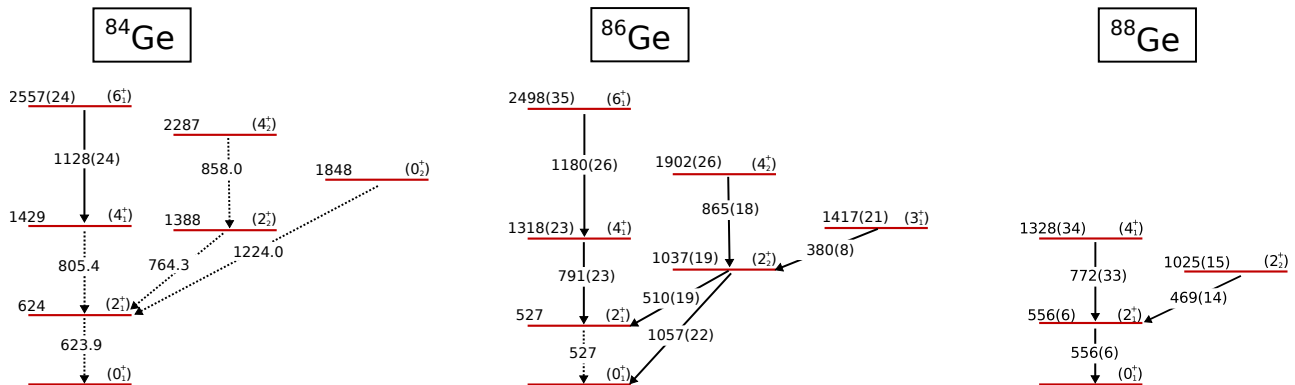


FIG. 2: Measured transition energies and proposed level energies of  $^{84,86,88}\text{Ge}$ . Dashed arrows denote transition energies taken from literature [32–35] and solid arrows mark transitions measured for the first time. The tentative spin assignments for  $^{84}\text{Ge}$  are taken from [32] (see text).

ror of 1.5 keV and an energy resolution of 9% and 6% FWHM at 662 keV and 1.332 MeV was obtained, respectively, which is in agreement with the analyses from Refs. [41, 43].

The Doppler-corrected  $\gamma$ -ray spectra of  $^{84,86,88}\text{Ge}$  are shown in Fig. 1. Each energy spectrum is described by a least-squares fit based on spectral response functions and lineshapes obtained from Monte-Carlo simulations, and a two-component exponential background. Derived transition energies have errors consisting of three contributions: the uncertainty of the energy calibration, the statistical error from the fitting procedure, and an error arising from the lifetime-dependent Doppler broadening and shift of the observed lineshapes. Upper limits of the lifetimes were derived by a  $\chi^2$  analysis while the error of the upper limit lifetime was obtained in a  $1\text{-}\sigma$  region of confidence. The derived upper limits are compatible with suggestions from the applied theories below.

$^{84}\text{Ge}$  was populated by the  $^{85}\text{Ge}(p,pn)$  reaction and, with a number of known  $\gamma$ -rays from  $\beta$ -delayed spectroscopy [32–34] served as a check for the spectral analysis. Six transitions at energies of 629(7) keV, 772(18) keV, 813(10) keV, 867(13) keV, 1128(24) keV and 1229(15) keV were identified (see Fig. 1 (a)), the 1128-keV transition for the first time. The other five transitions are in good agreement with Ref. [32], and a proposed level scheme is shown in Fig. 2. The present experiment is not sensitive to the spins of the involved states. However, based on systematics in neighboring Ge isotopes, we assign the newly observed 1128(24) keV  $\gamma$ -ray to the  $6_1^+ \rightarrow 4_1^+$  transition. The inset of Fig. 1 (a) shows the result of a coincidence condition on the  $2_1^+ \rightarrow 0_1^+$  transition. The 629(7) keV transition still appears due to coincidences with Compton events of higher-lying transition energies, but is largely reduced.

$^{86}\text{Ge}$  was populated by the  $^{87}\text{As}(p,2p)$  reaction, and the obtained Doppler-corrected spectrum is shown in Fig. 1 b). Seven transitions at energies 380(8) keV,

510(19) keV, 534(8) keV, 791(23) keV, 865(18) keV, 1057(22) keV and 1180(26) keV were measured. Only the 534(8)-keV transition has formerly been observed following  $\beta$  decay [35] and assigned to the decay of the  $2_1^+$  state, in agreement with the present data. A proposed level scheme of  $^{86}\text{Ge}$  is presented in Fig. 2, based on the following observations. For even-even nuclei populated in (p,2p) reactions (see, e.g., [44–47]), the strongest observed  $\gamma$  decay in the spectrum stems from the transition  $2_1^+ \rightarrow 0_1^+$ , while the second strongest intensity typically originates from the  $4_1^+ \rightarrow 2_1^+$  transition. The inset in Fig. 1 b) displays a  $\gamma\gamma$ -coincidence spectrum, gated on the energy range from 440 keV to 590 keV. A strong peak in the gated energy range remains due to the 510(19)/534(8) keV doublet. The peak at 1057(22) keV is not in coincidence with the gated energy range. We assign this transition as the ground state transition of a  $2^+$  state at 1057(22) keV. The fitted energies of the doublet, 510(19) keV and 534(8) keV, sum up to 1057(22) keV within error. Therefore, we assign the 510(19)-keV  $\gamma$ -ray to the  $2_2^+ \rightarrow 2_1^+$  transition. The transitions at 865(18) keV and 1180(26) keV are assigned to be  $6_1^+ \rightarrow 4_1^+$  and  $4_2^+ \rightarrow 2_2^+$ , respectively, based on comparison to  $^{84}\text{Ge}$ . A standard significance test [48] for the 380-keV peak yields  $\sim 4\sigma$  in singles and  $> 2\sigma$  in the gated spectra. This transition appears in the gate on the  $\sim 520$ -keV doublet, as well as weakly in the gate on the 1060-keV region where the  $2_2^+ \rightarrow 0_1^+$  transition is expected, whereas a gate on a neighboring ( $\sim 1360$ -keV) region yields no 380-keV peak (see Fig. 1 (b)). As discussed further below this transition is tentatively assigned to the  $3_1^+ \rightarrow 2_2^+$  transition.

The Doppler-corrected  $\gamma$ -spectrum from the reaction  $^{89}\text{As}(p,2p)^{88}\text{Ge}$  is shown in Fig. 1 c). The three  $\gamma$ -ray transitions at energies 469(14) keV, 556(6) keV and 772(33) keV are observed for the first time. A suggested level scheme of  $^{88}\text{Ge}$  is presented in Fig. 2. The transition at 556(6) keV has the strongest intensity indicating a

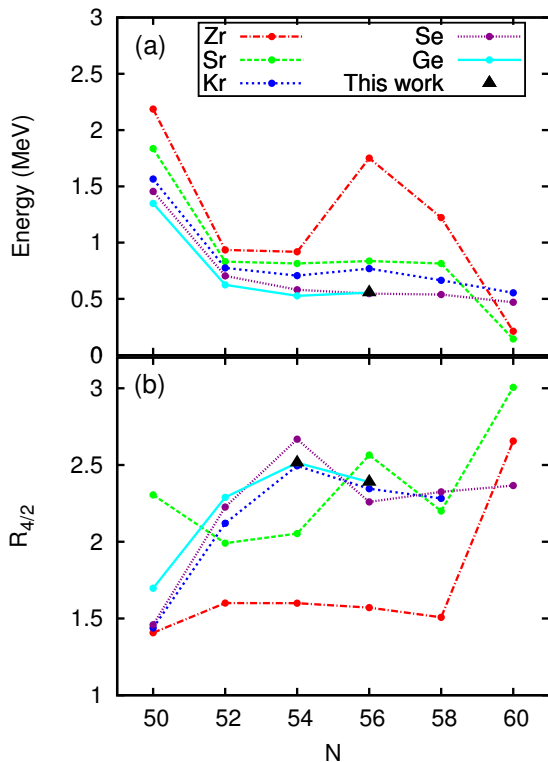


FIG. 3: (a) Behavior of the  $2_1^+$  energies for the isotopic chains of Zr ( $Z = 40$ ), Sr ( $Z = 38$ ), Kr ( $Z = 36$ ), Se ( $Z = 34$ ) and Ge ( $Z = 32$ ). (b) Trend of the  $R_{4/2}$ -ratios of the same isotopic chains.

$2_1^+ \rightarrow 0_1^+$  transition. The  $\gamma$ -ray at 772(33) keV is assigned to the  $4_1^+ \rightarrow 2_1^+$  transition, and the  $\gamma$ -ray at 469 keV is assigned to the  $2_2^+ \rightarrow 2_1^+$  transition from comparison to neighboring  $^{86}\text{Ge}$  and  $^{90}\text{Se}$  [49]. A gate on the  $2_1^+ \rightarrow 0_1^+$  transition (see inset of Fig. 1 (c)) yields both transitions.

The trends of the  $2_1^+$  energies for even-even nuclei from Zr ( $Z = 40$ ) to Ge ( $Z = 32$ ) are depicted in Fig. 3 (a). In zirconium isotopes the  $2_1^+$  energy peaks at  $N = 56$ . It maintains a rather high value at  $N = 58$  before it significantly drops at the onset of collectivity at  $N = 60$ . For Sr [50], Kr [51] and Se [49] isotopes no such peaking of the  $2_1^+$  energies is found, but rather a flat behavior up to  $N = 58$ . Nevertheless, a slight increase in the  $2_1^+$  energy at  $N = 56$  is observed for  $^{92}\text{Kr}$  and  $^{88}\text{Ge}$  (this work). The ratios  $R_{4/2} = E(4_1^+)/E(2_1^+)$  for the same isotopic chains are shown in Fig. 3 (b). The systematic trend in the Ge isotopic chain is very similar to those in the Kr and Se isotopic chains, but significantly different from the Zr and Sr isotopic chains. An increase of the  $R_{4/2}$  ratio from  $N = 50$  to  $N = 54$ , followed by a drop toward  $N = 56$  is observed. The flat behavior of  $2_1^+$  energies from  $Z = 38$  (Sr) down to  $Z = 32$  (Ge), along with the  $R_{4/2}$  trend, may indicate a remainder of the  $N = 56$  sub-shell closure, or a small fluctuation in their collective structure. All  $^{84,86,88}\text{Ge}$  isotopes have  $R_{4/2}$  ratios around 2.5, which is typical for  $O(6)$ -like,  $\gamma$ -soft nuclei.

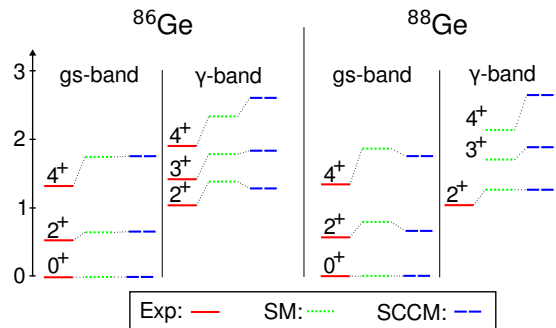


FIG. 4: Systematics of the obtained level energies from  $^{86,88}\text{Ge}$  by experiment compared to theoretical predictions from shell model (SM) and SCCM.

In the following the experimental results are compared to shell model calculations and a symmetry-conserving configuration mixing Gogny (SCCM) calculation. For more details on these calculations, and including a shell model calculation for  $^{84}\text{Ge}$ , we refer to Ref. [27] and references therein. Fig. 4 shows the observed excited states of  $^{86,88}\text{Ge}$  and compares the results to the predictions from both theories. The predicted sequence of the states is in good agreement with the proposed ones from data, although excitation energies are overestimated in all cases. For both nuclei the predicted  $R_{4/2}$  ratios are in the range of  $\sim 2.5$ , which agrees with the values obtained from experiment. The low-lying  $\gamma$ -band in both sets of calculations reflects a degree of triaxiality in both isotopes. Furthermore, both theories predict a  $3_1^+$  state which is closer to the  $2_2^+$  state than to the  $4_2^+$  state in the  $\gamma$ -band. A promising candidate for this state is observed in the present experiment through the 380(8)-keV transition, since the strongest decay from the  $3_1^+$  state is expected to be to the  $2_2^+$  state. Although an excited  $0^+$  state is predicted in this energy range, we stress that it would dominantly decay to the  $2_1^+$  state. In the present experiments, such a transition is observed only for  $^{84}\text{Ge}$ , not for  $^{86}\text{Ge}$ . This leads to the tentative  $J = 3$  assignment, which has an important consequence, as discussed below.

The staggering in the  $\gamma$ -band [20]

$$S(J) = \frac{[E(J) - E(J-1)] - [E(J-1) - E(J-2)]}{E(2_1^+)} \quad (1)$$

should take positive values for a rigid triaxial nucleus. Note that this will trivially be the case also for a well-deformed rotor with  $E(J) \propto J(J+1)$ . However, in such a case the position of the band head of the  $\gamma$  band is much higher relative to the yrast states. In the only known case of a nucleus with rigid triaxial deformation in the ground state,  $^{76}\text{Ge}$ ,  $S(4) = 0.091(2)$  has been found. With the assignments in the present work, for  $^{86}\text{Ge}$  a value of  $S(4) = 0.20(9)$  results, pointing at an even larger degree of triaxiality in the ground state. Comparing the level

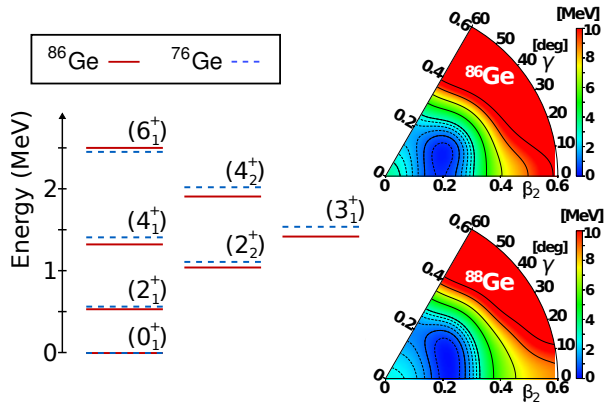


FIG. 5: (left) Comparison of the low spin spectrum of  $^{76}\text{Ge}$  (blue, dashed) and  $^{86}\text{Ge}$  (red, solid). (right) Potential energy surfaces in the particle number variation after projection (PN-VAP) approach [55] for  $^{86}\text{Ge}$  (top) and  $^{88}\text{Ge}$  (bottom). The spacing between solid contour lines is 2 MeV with intermediate dashed lines for 0.5 MeV steps.

schemes of  $^{86}\text{Ge}$  and  $^{76}\text{Ge}$ , there are strong similarities, as shown in Fig. 5; the level energies agree within 100 keV. Especially the relative positions of the odd- to the even-spin  $\gamma$ -band members appear to be consistent. This matches very well the predictions from both models considered, shell model and SCCM (see Fig. 4). Examining the potential energy surfaces from the SCCM calculations (see Fig. 5), a triaxial minimum is found for  $^{86}\text{Ge}$ , and  $^{88}\text{Ge}$  is predicted very similar, with a somewhat larger  $\beta$  deformation and more  $\gamma$  softness. In both calculations, the wave functions of the low-lying states maximize at triaxial values. Similar conclusions are drawn from the shell model calculations. From an analysis of E2 matrix elements, i.e., the use of quadrupole shape invariants [52], we derive an invariant  $K_3$  of 0.027 for both,  $^{86,88}\text{Ge}$ , in the SCCM, corresponding to an effective  $\gamma$  value of  $29.5^\circ$  near maximum triaxiality. However, the fluctuations of  $K_3$  are very different for  $^{86,88}\text{Ge}$ , that is 0.01 and 0.13, respectively, which reflects the large degree of triaxial rigidity in  $^{86}\text{Ge}$ . Similarly, the shell model yields large triaxiality for both isotopes, and fluctuations in  $K_3$  are an order of magnitude larger in  $^{88}\text{Ge}$  than in  $^{86}\text{Ge}$ . We note that different cut-offs in the sums for deriving the shape invariants give consistent results, similar to previous works [53, 54].

To conclude,  $\gamma$ -spectroscopy of neutron-rich Ge isotopes has been performed, for the first time of  $^{88}\text{Ge}$ . 16 transitions in  $^{84,86,88}\text{Ge}$  have been observed ten of which so far unknown. On the basis of the observed intensities and systematics in neighboring Ge isotopes new level schemes for  $^{86,88}\text{Ge}$  are proposed for the first time. The tentative assignment of a  $3_1^+$  state in  $^{86}\text{Ge}$  would

be compatible to new model predictions, as well as to typical collective-model level orderings. This points to a degree of rigid triaxiality in this nucleus, which has previously been predicted within this broader mass region. New calculations predict a maximum of triaxiality in  $^{86}\text{Ge}$ . Our measurements show the first indication of rigid ground state triaxiality in this very neutron-rich region of the nuclear chart.  $^{86}\text{Ge}$  may constitute the first example of an unstable nucleus with this feature in this newly-accessible region which is much discussed in view of triaxial features, as well as shape coexistence. A study of ESPEs like in  $^{110}\text{Zr}$  [29] may shed light on the possibility of the emergence of triaxiality as the result of the bunching of single-particle orbitals.

The authors thank the RIBF and BigRIPS teams for providing a stable, high-intensity uranium beam and operating the secondary beams. We acknowledge support from the German BMBF Grant Nos. 05P12RDFN8 and 05P15PKFNA, the ERC Grant No. MINOS-258567, the Spanish Ministerio de Economía y Competitividad under contracts FPA2014-57196-C5-4-P and FIS-2014-53434, the Vietnam Ministry of Science and Technology, as well as from the Science and Technology Facilities Council (STFC). We further thank GSI for providing computing facilities.

\* mlettman@ikp.tu-darmstadt.de

- [1] A. Bohr and B. Mottelson, Mat. Fys. Medd. Dan. Vid. Selsk. **27** (1953).
- [2] A. S. Davydov and G. F. Filippov, Nucl. Phys. **8**, 237 (1958).
- [3] L. Wilets and M. Jean, Phys. Rev. **102**, 788 (1956).
- [4] M. Göppert-Mayer, Phys. Rev. **75**, 1969 (1949).
- [5] M. Göppert-Mayer and J. H. D. Jensen, *Elementary Theory of Nuclear Shell Structure* (Wiley, New York, 1955).
- [6] F. Iachello and A. Arima, *The interacting boson model* (Cambridge University Press, Cambridge, 1987).
- [7] M. Bender, P.-H. Heenen, and P.-G. Reinhard, Rev. Mod. Phys. **75**, 121 (2003).
- [8] T. R. Rodríguez and J. L. Egido, Phys. Rev. C. **81**, 064323 (2010).
- [9] S. W. Ødegård, G. B. Hagemann, D. R. Jensen, M. Bergström, B. Herskind, G. Sletten, S. Törmänen, J. N. Wilson, P. O. Tjøm, I. Hamamoto, et al., Phys. Rev. Lett. **86**, 5866 (2001).
- [10] D. J. Hartley, R. V. F. Janssens, L. L. Riedinger, M. A. Riley, A. Aguilar, M. P. Carpenter, C. J. Chiara, P. Chowdhury, I. G. Darby, U. Garg, et al., Phys. Rev. C **80**, 041304(R) (2009).
- [11] G. Schonwasser, H. Hubel, G. B. Hagemann, P. Bednarczyk, G. Benzoni, A. Bracco, P. Bringel, R. Chapman, D. Curien, J. Domscheit, et al., Phys. Lett. B **552**, 9 (2003).
- [12] S. Frauendorf and J. Meng, Nucl. Phys. A **617**, 131 (1997).
- [13] T. Koike, K. Starosta, and I. Hamamoto, Phys. Rev. Lett. **93**, 172502 (2004).

- [14] K. Starosta, T. Koike, C. J. Chiara, D. B. Fossan, and D. R. LaFosse, Nucl. Phys. A **682**, 375c (2001).
- [15] D. Tonev, G. de Angelis, P. Petkov, A. Dewald, S. Brant, S. Frauendorf, D. L. Balabanski, P. Pejovic, D. Bazzacco, P. Bednarczyk, et al., Phys. Rev. Lett. **96**, 052501 (2006).
- [16] J. A. Cizewski, R. F. Casten, G. J. Smith, M. L. Stelts, W. R. Kane, H. G. Börner, and W. F. Davidson, Phys. Rev. Lett. **40**, 167 (1978).
- [17] J. Jolie, J. M. Régis, D. Wilmsen, N. Saed-Samii, M. Pfeiffer, N. Warr, A. Blanc, M. Jentschel, U. Köster, P. Mutti, et al., Nucl. Phys. A **934**, 1 (2015).
- [18] N. Pietralla, T. Möller, C. J. Lister, E. A. McCutchan, G. Rainovski, C. Bauer, M. P. Carpenter, R. V. F. Janssens, D. Seweryniak, and S. Zhu, EPJ Web of Conferences **93**, 01002 (2015).
- [19] S. Bhattacharyya, M. Rejmund, A. Navin, E. Caucier, F. Nowacki, A. Poves, R. Chapman, D. O'Donnell, M. Gelin, A. Hodsdon, et al., Phys. Rev. Lett. **101**, 032501 (2008).
- [20] N. V. Zamfir and R. F. Casten, Phys. Lett. B **260**, 265 (1991).
- [21] E. A. McCutchan, D. Bonatsos, N. V. Zamfir, and R. F. Casten, Phys. Rev. C **76**, 024306(R) (2007).
- [22] Y. Toh, C. J. Chiara, E. A. McCutchan, W. B. Walters, R. V. F. Janssens, M. P. Carpenter, S. Zhu, R. Broda, B. Fornal, B. P. Kay, et al., Phys. Rev. C **87**, 041304(R) (2013).
- [23] S. F. Shen, S. J. Zheng, F. R. Xu, and R. Wyss, Phys. Rev. C **84**, 044315(R) (2011).
- [24] J. J. Sun, Z. Shi, X. Q. Li, H. Hua, C. Xu, Q. B. Chen, S. Q. Zhang, C. Y. Song, J. Meng, X. G. Wu, et al., Phys. Lett. B **734**, 308 (2014).
- [25] T. Nikšić, P. Marević, and D. Vretenar, Phys. Rev. C **89**, 044325 (2014).
- [26] Zhang, D. -L. and Ding, B. -G., Chin. Phys. Lett. **30**, 122101(R) (2013).
- [27] K. Sieja, T. R. Rodríguez, K. Kolos, and D. Verney, Phys. Rev. C **88**, 034327(R) (2013).
- [28] M. Lebois, D. Verney, F. Ibrahim, S. Essabaa, F. Azaiez, M. Cheikh Mhamed, E. Cottureau, P. V. Cuong, M. Ferraton, K. Flanagan, et al., Phys. Rev. C **80**, 044308(R) (2009).
- [29] T. Togashi, Y. Tsunoda, T. Otsuka, and N. Shimizu, Phys. Rev. Lett. **117**, 172502 (2016).
- [30] L. Guo, J. A. Maruhn, and P.-G. Reinhard, Phys. Rev. C **76**, 034317(R) (2007).
- [31] S. Hilaire and M. Girod, *Cea*, <http://www-phynu.cea.fr>, accessed: 2016-11-08.
- [32] A. Korgul, K. P. Rykaczewski, R. Grzywacz, H. Śliwińska, J. C. Batchelder, C. Bingham, I. N. Borzov, N. Brewer, L. Cartegni, A. Fijałkowska, et al., Phys. Rev. C **88**, 044330 (2013).
- [33] K. Kolos, D. Verney, F. Ibrahim, F. Le Blanc, S. Franchoo, K. Sieja, F. Nowacki, C. Bonnin, M. Cheikh Mhamed, P. V. Cuong, et al., Phys. Rev. C **88**, 047301 (2013).
- [34] J. A. Winger, K. P. Rykaczewski, C. J. Gross, R. Grzywacz, J. C. Batchelder, C. Goodin, J. H. Hamilton, S. V. Ilyushkin, A. Korgul, W. Królas, et al., Phys. Rev. C **81**, 044303 (2010).
- [35] K. Miernik, K. P. Rykaczewski, C. J. Gross, R. Grzywacz, M. Madurga, D. Miller, J. C. Batchelder, I. N. Borzov, N. T. Brewer, C. Jost, et al., Phys. Rev. Lett. **111**, 132502 (2013).
- [36] P. Doornenbal and A. Obertelli, RIKEN proposal for scientific program p. unpublished (2013).
- [37] C. Santamaria, C. Louchart, A. Obertelli, V. Werner, P. Doornenbal, F. Nowacki, G. Authalet, H. Baba, D. Calvet, F. Château, et al., Phys. Rev. Lett. **115**, 192501 (2015).
- [38] T. Kubo, D. Kameda, H. Suzuki, N. Fukuda, H. Takeda, Y. Yanagisawa, M. Ohtake, K. Kusaka, K. Yoshida, N. Inabe, et al., Prog. Theor. Exp. Phys. p. 03C003 (2012).
- [39] N. Fukuda, T. Kubo, T. Ohnishi, N. Inabe, H. Takeda, D. Kameda, and H. Suzuki, Nucl. Instrum. Methods Phys. Res. B **317**, 323 (2013).
- [40] A. Obertelli, A. Delbart, S. Anvar, L. Audirac, G. Authalet, H. Baba, B. Bruyneel, D. Calvet, F. Château, A. Corsi, et al., Eur. Phys. J. A **50**, 8 (2014).
- [41] S. Takeuchi, T. Motobayashi, Y. Togano, M. Matsushita, N. Aoi, K. Demichi, H. Hasegawa, and H. Murakami, Nucl. Instrum. Methods Phys. Res. A **763**, 596 (2014).
- [42] S. Agostinelli, J. Allison, K. Amako, J. Apostolakis, H. Araujo, P. Arce, M. Asai, D. Axen, S. Banerjee, G. Barrand, et al., Nucl. Instrum. Methods Phys. Res. A **506**, 250 (2003).
- [43] P. Doornenbal, Prog. Theor. Exp. Phys. p. 03C004 (2012).
- [44] P. Doornenbal, H. Scheit, S. Takeuchi, N. Aoi, K. Li, M. Matsushita, D. Steppenbeck, H. Wang, H. Baba, H. Crawford, et al., Phys. Rev. Lett. **111**, 212502 (2013).
- [45] H. Iwasaki, A. Lemasson, C. Morse, A. Dewald, T. Braunroth, V. M. Bader, T. Baugher, D. Bazin, J. S. Berryman, C. M. Campbell, et al., Phys. Rev. Lett. **112**, 142502 (2014).
- [46] D. Bazin, B. A. Brown, C. M. Campbell, J. A. Church, D. C. Dinca, J. Enders, A. Gade, T. Glasmacher, P. G. Hansen, W. F. Mueller, et al., Phys. Rev. Lett. **91**, 012501 (2003).
- [47] P. Fallon, E. Rodriguez-Vieitez, A. O. Macchiavelli, A. Gade, J. A. Tostevin, P. Adrich, D. Bazin, M. Bowen, C. M. Campbell, R. M. Clark, et al., Phys. Rev. C **81**, 041302 (2010).
- [48] K. Weise, K. Hübel, E. Rose, M. Schläger, D. Schrammel, M. Täschner, and R. Michel, Radiat Prot Dosimetry **121**, 52 (2006).
- [49] S. Chen, P. Doornenbal, A. Obertelli, T. R. Rodríguez, G. Authalet, H. Baba, D. Calvet, F. Château, A. Corsi, A. Delbart, et al., submitted to Phys. Lett. B (2016).
- [50] Negret, A. and Sonzogni, A. A., ENSDF (2011).
- [51] C. M. Baglin, NDS **113**, 2187 (2012).
- [52] V. Werner, N. Pietralla, P. von Brentano, R. F. Casten, and R. V. Jolos, Phys. Rev. C **61**, 021301 (2000).
- [53] V. Werner, P. von Brentano, and R. V. Jolos, Phys. Lett. B **521**, 146 (2001).
- [54] V. Werner, C. Scholl, and P. von Brentano, Phys. Rev. C **71**, 054314 (2005).
- [55] M. Anguiano, J. Egido, and L. Robledo, Phys. Lett. B **545**, 62 (2002).